Journal of Control, Automation and Electrical Systems (2018) 29:22–31
https://doi.org/10.1007/s40313-017-0351-x

Design of Coordinated Decentralized Damping Controllers for Power Systems Considering Uncertainties

Murilo E. C. Bento[1] · Daniel Dotta[2] · Roman Kuiava[3] · Rodrigo A. Ramos[1]

Received: 14 June 2017 / Revised: 6 November 2017 / Accepted: 19 November 2017 / Published online: 29 November 2017

Abstract
This paper presents an analytical method based on the solution of the nonlinear Riccati equation for the design of coordinated, decentralized damping controllers for power systems. While other approaches use analytical methods that ensure robustness with respect to uncertainties in the system operating conditions by considering a controller of the same order as the plant, which results in high-order controller structures, the proposed method has the advantage of providing robust and decentralized low-order controllers. The method is applied to two IEEE benchmarks, and the designed controllers are assessed by modal analysis and nonlinear time-domain simulation.

Keywords Power system small-signal stability · Uncertainties · Riccati equation

1 Introduction

The small-signal stability problem in power systems must be considered to avoid undesirable and very costly events such as blackouts and severe constraints in the power transfer capacity of transmission lines. In recent years, the power system industry has undergone a strong infrastructure change with the addition of new generation facilities such as wind farms and solar photovoltaic (PV) plants with complex power electronic controls, growing system loads or the retirement of large generating stations. These new components may also introduce uncertainties in the system operating conditions due to such factors as random fluctuations of the wind and PV power generation. As a result, the operating point of the whole power system changes more often through generation random variations. These can create adverse effects on the system's dynamic stability and make the damping control design more difficult (Galvan and Overholt 2014; Bian et al. 2016).

On the other hand, the power electronics interface in use for some types of generation and storage technologies, such as battery or flywheel (Ortega and Milano 2016) and wind turbines (Wilches-Bernal et al. 2016), together with advance monitoring, such as wide area measurement systems (WAMS), can improve the power system's observability and controllability. In this context, the development of methods for the coordinated design of robust damping controllers is necessary to ensure optimal and reliable operation of modern power systems (Annaswamy and Amin 2013). That is why (Canizares 2017) were motivated to create benchmark models for evaluating decentralized control design methods.

The literature proposes a great number of approaches for the design of coordinated, robust damping controllers for power systems. These approaches can be divided into two basic types: evolution-based search (Do Bomfim et al. 2000; Castoldi et al. 2014; Lu et al. 2013; Shahgholian and Movahedi 2016) and optimization/search analytical methods (Deng and Zhang 2014; Elkington and Ghandhari 2013; Ramos et al. 2004).

Evolution-based search methods are able to construct new control laws and nonintuitive solutions. The major drawbacks for applying evolutionary-based methods such as genetic algorithms and particle swarm optimization for the power system are their computational burden and the lack of a

This work was financially supported by FAPESP under Grant Nos. 2015/02569-6, 2015/24245-8, 2015/18806-7 and 2016/08645-9.

✉ Murilo E. C. Bento
murilo.bento@usp.br

[1] University of Sao Paulo, Av. Trabalhador Sao-Carlense, 400, Sao Carlos, SP 13566-330, Brazil

[2] State University of Campinas, Av. Albert Einstein, 970, Campinas, SP 13083-852, Brazil

[3] Federal University of Parana, Rua Cel, Francisco Heraclito dos Santos, Curitiba, PR 81531-980, Brazil

formal performance guarantee based on quadratic stability.

The analytical methods can be further subdivided into two categories: linear matrix inequalities (LMIs) and Riccati equation or linear quadratic regulator (LQR) problems. The LMIs became popular in the 1990s, because they can guarantee when the problem would become convex, global optimal solution considering uncertainties that belong to a polytopic domain. However, the major drawbacks of convexity are as follows: (i) the conservatism derived from the LMI conditions; (ii) the high dimensionality of the designed controllers; (iii) the presence of Lyapunov variables, which grow quadratically with the system size when the robust stabilization of the uncertain system is based on quadratic stability. The practical result of these limitations is that the current LMI solvers quickly break down when plants get sizeable.

On the other hand, the Riccati equation methods have the major advantage in their capacity to treat a large-scale system, such as presented in the work of Costa et al. (1997). The main issues related to this method are the capacity of considering uncertainties and the numerical convergence success (Apkarian et al. 2007).

The main contribution of this paper is its application of the method based on the solution of the Riccati equation considering system's operating uncertainties, as originally proposed in Trinh and Aldeen (1993), for the challenging problem of designing coordinated and robust decentralized power system stabilizers (PSSs). The resulting decentralized controllers present a fixed and low-order structure that allows for practical implementation. Quadratic stability over the required range of uncertainties is also guaranteed for the power system with the designed controllers.

To ensure that controller performance is properly compared, the analysis includes two test systems presented in IEEE standard benchmark models (Canizares 2017). Small-signal stability analysis and nonlinear time-domain simulations are used to validate the design and assess its performance in the multimachine Southern/Southeastern Brazilian equivalent and a 39 New England power systems.

The paper is organized as follows. Section 2 presents the power system modeling and control structure. The design method is presented in Sect. 3. Section 4 describes the application of this method for power system control design. In Sect. 5, the performance evaluation for the damping controllers designed by the proposed technique is performed via small-signal stability analysis, time-domain nonlinear simulations and a comparative analysis with the stabilizers originally designed for the two adopted test systems. Section 6 includes the conclusion and final comments.

2 The Power System and Decentralized Controller Models

2.1 The Power System Model

Most of the damping control design methods for power systems are based on the following state-space system (Kundur 1994):

$$\dot{\mathbf{x}} = (\mathbf{A} + \Delta\mathbf{A})\mathbf{x} + \mathbf{B}\mathbf{u} \tag{1}$$

$$\mathbf{y} = \mathbf{C}\mathbf{x} \tag{2}$$

where $\mathbf{x} \in \Re^n$, $\mathbf{u} \in \Re^p$ and $\mathbf{y} \in \Re^p$ are the state, input and output vectors, respectively. Matrices $\mathbf{A}$ and $\Delta\mathbf{A}$ are of proper dimensions, where $\mathbf{A}$ comes from the linearization process on the power system nonlinear model with respect to a selected operating point, while $\Delta\mathbf{A}$ represents the prescribed range of uncertainties. No uncertainty is associated with the control input matrix $\mathbf{B}$; furthermore, p is the number of decentralized controllers to be designed.

Matrices $\mathbf{A}$ and $\mathbf{\Delta A}$ are presented

$$\mathbf{A} = \begin{bmatrix} a_{11} & \cdots & a_{1j} & \cdots & a_{1n} \\ \vdots & \ddots & \vdots & \ddots & \vdots \\ a_{i1} & \cdots & a_{ij} & \cdots & a_{in} \\ \vdots & \ddots & \vdots & \ddots & \vdots \\ a_{n1} & \cdots & a_{nj} & \cdots & a_{nn} \end{bmatrix} \tag{3}$$

$$\mathbf{\Delta A} = \begin{bmatrix} \Delta a_{11} & \cdots & \Delta a_{1j} & \cdots & \Delta a_{1n} \\ \vdots & \ddots & \vdots & \ddots & \vdots \\ \Delta a_{i1} & \cdots & \Delta a_{ij} & \cdots & \Delta a_{in} \\ \vdots & \ddots & \vdots & \ddots & \vdots \\ \Delta a_{n1} & \cdots & \Delta a_{nj} & \cdots & \Delta a_{nn} \end{bmatrix} \tag{4}$$

2.2 The Decentralized Controller

In order to design a set of p decentralized controllers for the system represented by (1) and (2), the structure adopted for each controller is based on dynamic output feedback control. It is possible to describe the set of p controllers in the compact form in state space as follows:

$$\dot{\mathbf{x}}_\mathbf{c} = \mathbf{A}_\mathbf{c}\mathbf{x}_\mathbf{c} + \mathbf{B}_\mathbf{c}\mathbf{y} \tag{5}$$

$$\mathbf{u} = \mathbf{C}_\mathbf{c}\mathbf{x}_\mathbf{c} + \mathbf{D}_\mathbf{c}\mathbf{y} \tag{6}$$

where $\mathbf{x_c}$ is the vector with the states of the controllers and $\mathbf{u}$ and $\mathbf{y}$ come from (1) and (2). A decentralized structure of the controllers is guaranteed by adoption of a block-diagonal

structure to the transfer function matrix $\mathbf{DC}(s)$ obtained from (5) and (6), which is given by the following:

$$\mathbf{DC}(s) = \mathbf{C_c}(s\mathbf{I} - \mathbf{A_c})^{-1}\mathbf{B_c} + \mathbf{D_c} \tag{7}$$

$$= \begin{bmatrix} dc_1(s) & 0 & \cdots & 0 \\ 0 & dc_2(s) & \cdots & 0 \\ \vdots & \vdots & \ddots & \vdots \\ 0 & 0 & \cdots & dc_p(s) \end{bmatrix} \tag{8}$$

In this paper, each decentralized controller $dc_i(s)$ is described by a second-order transfer function

$$dc_i(s) = \frac{n_2^i s^2 + n_1^i s + n_0^i}{s^2 + a_1^i s + a_0^i} = \frac{b_1^i s + b_0^i}{s^2 + a_1^i s + a_0^i} + d^i \tag{9}$$

where $d^i = n_2^i$, $b_0^i = n_0^i - n_2^i a_0^i$ and $b_1^i = n_1^i - n_2^i a_1^i$. Notice that the chosen structure for the damping controller is similar in format to the ones adopted in industrial implementations.

From (9), the observable canonical form of the matrices $\mathbf{A_c}$, $\mathbf{B_c}$, $\mathbf{C_c}$ and $\mathbf{D_c}$ can be described by

$$\mathbf{A_c} = \begin{bmatrix} \mathbf{A}_{c_1} & \cdots & 0 \\ \vdots & \ddots & \vdots \\ 0 & \cdots & \mathbf{A}_{c_p} \end{bmatrix}, \quad \mathbf{B_c} = \begin{bmatrix} \mathbf{B}_{c_1} & \cdots & 0 \\ \vdots & \ddots & \vdots \\ 0 & \cdots & \mathbf{B}_{c_p} \end{bmatrix}, \tag{10}$$

$$\mathbf{C_c} = \begin{bmatrix} \mathbf{C}_{c_i} & \cdots & 0 \\ \vdots & \ddots & \vdots \\ 0 & \cdots & \mathbf{C}_{c_p} \end{bmatrix}, \quad \mathbf{D_c} = \begin{bmatrix} d^1 & \cdots & 0 \\ \vdots & \ddots & \vdots \\ 0 & \cdots & d^p \end{bmatrix} \tag{11}$$

where $\mathbf{A}_{c_i}$, $\mathbf{B}_{c_i}$ and $\mathbf{C}_{c_i}$, $\quad i = 1, \ldots, p$, are given by

$$\mathbf{A}_{c_i} = \begin{bmatrix} 1 & -a_0^i \\ 0 & -a_1^i \end{bmatrix}, \quad \mathbf{B}_{c_i} = \begin{bmatrix} b_0^i \\ b_1^i \end{bmatrix}, \quad \mathbf{C}_{c_i} = \begin{bmatrix} 0 & 1 \end{bmatrix} \tag{12}$$

The next subsection discusses the closed-loop system obtained from power system model (1) and (2) and decentralized controllers (5) and (6).

2.3 The Closed-Loop System

Let the closed-loop system formed by the interconnection of system Eqs. (1) and (2) with the controllers in state-space form (5) and (6), be described as

$$\dot{\bar{\mathbf{x}}} = \bar{\mathbf{A}}\bar{\mathbf{x}} \tag{13}$$

where $\bar{\mathbf{x}} = \begin{bmatrix} \mathbf{x}^{\mathrm{T}} & \mathbf{x_c}^{\mathrm{T}} \end{bmatrix}^{\mathrm{T}}$ and

$$\bar{\mathbf{A}} = \begin{bmatrix} \mathbf{A} + \mathbf{B}\mathbf{D_c}\mathbf{C} & \mathbf{B}\mathbf{C_c} \\ \mathbf{B_c}\mathbf{C} & \mathbf{A_c} \end{bmatrix} \tag{14}$$

Then, by defining the matrices

$$\mathbf{A_a} = \begin{bmatrix} \mathbf{A} & \mathbf{B}\mathbf{C_c} \\ \mathbf{0} & \mathbf{A_c} \end{bmatrix}, \quad \mathbf{B_a} = \begin{bmatrix} \mathbf{B} & \mathbf{0} \\ \mathbf{0} & \mathbf{I} \end{bmatrix}, \tag{15}$$

$$\mathbf{C_a} = \begin{bmatrix} \mathbf{C} & \mathbf{0} \end{bmatrix}, \quad \mathbf{G_a} = \begin{bmatrix} -\mathbf{D_c} & -\mathbf{B_c} \end{bmatrix}^{\mathrm{T}} \tag{16}$$

and the augmented state vector $\mathbf{x_a} = \begin{bmatrix} \mathbf{x}^{\mathrm{T}} & \mathbf{x_c}^{\mathrm{T}} \end{bmatrix}^{\mathrm{T}}$, an augmented system can be obtained by

$$\dot{\mathbf{x}}_\mathbf{a} = \mathbf{A_a}\mathbf{x_a} + \mathbf{B_a}\mathbf{u_a} \tag{17}$$

$$\mathbf{y_a} = \mathbf{C_a}\mathbf{x_a} \tag{18}$$

where the closed-loop system given by (13) is equivalent to the augmented system given by (17) and (18) with the output feedback control law given by

$$\mathbf{u_a} = -\mathbf{G_a}\mathbf{C_a}\mathbf{x_a} = -\mathbf{G_a}\mathbf{y_a} \tag{19}$$

If the observable canonical form is used to represent the controller in (5) and (6) and if the poles of the controllers are fixed, matrices $\mathbf{A_a}$, $\mathbf{B_a}$ and $\mathbf{C_a}$ are known. Matrices $\mathbf{D_c}$ and $\mathbf{B_c}$, corresponding to the gain and zeros of the decentralized controllers, must be determined from the static output gains given by matrix $\mathbf{G_a}$. Therefore, the output dynamic feedback control problem is reduced to a constant output feedback problem (Costa et al. 1997) given by the computation of control law (19) (that is, the matrix $\mathbf{G_a}$). This fact is explored by the control design methodology, which is discussed in the next section.

3 Control Design Method Incorporating System Uncertainties

The proposed methodology is based on the linear quadratic regulator (LQR) and aims to determine a time-invariant feedback gain matrix. The resulting decentralized output feedback controller is robust and satisfies power system damping requirements. The unconstrained linear quadratic problem, represented by closed-loop system (17), has an unique optimal solution for the state feedback control law given by

$$\mathbf{u_a} = -\mathbf{K}\mathbf{x_a} \tag{20}$$

where $\mathbf{K}$ is the state feedback gain and must satisfy

$$\mathbf{K} = \mathbf{R}^{-1}\mathbf{B}^{\mathbf{T}}\mathbf{P} \tag{21}$$

and $\mathbf{P}$ is a symmetric positive definite solution of well-known Riccati equation (Geromel and Peres 1985). So, from the computation of matrix $\mathbf{K}$, by (21), determines state feedback control law (20). In the next subsection, the LQR method is extended to solve the output feedback control problem given by (17)–(19) with the imposition of block-diagonal structures for the controller matrices.

3.1 Decentralization and Output Feedback

The decentralization constraint is satisfied with a block-diagonal structure for the matrices $\mathbf{K}$, $\mathbf{D_c}$ and $\mathbf{B_c}$ (Geromel and Peres 1985). The inclusion of the output feedback constraint is more demanding than decentralization, as described in Geromel and Peres (1985). In order to fulfill the output feedback constraint as imposed by (19), Geromel and Peres (1985) showed that every $\mathbf{K}$ can be written as

$$\mathbf{K} = \mathbf{K}\mathbf{C}_\mathbf{a}^\mathbf{T}(\mathbf{C_a}\mathbf{C}_\mathbf{a}^\mathbf{T})^{-\mathbf{1}}\mathbf{C_a} = \mathbf{G_a}\mathbf{C_a} \tag{22}$$

where

$$\mathbf{G_a} = \mathbf{K}\mathbf{C}_\mathbf{a}^\mathbf{T}(\mathbf{C_a}\mathbf{C}_\mathbf{a}^\mathbf{T})^{-\mathbf{1}} \tag{23}$$

Notice that the calculation of $\mathbf{G_a}$ from (23) determines the output control law in (19) and, consequently, the matrices $\mathbf{D_c}$ and $\mathbf{B_c}$ of the controllers.

3.2 Design Method Considering Uncertainties

Trinh and Aldeen (1993) showed that, for a given linear system described by (17) and (18) with system uncertainties that can be written to satisfy the following matching condition $\Delta\mathbf{A_a} = \mathbf{B_a}\mathbf{S}$, there is an arbitrary matrix $\mathbf{L}$ and a matrix $\mathbf{K}$, given by (22), which satisfy the following relationship

$$\mathbf{K} + \mathbf{L} = \mathbf{R}^{-\mathbf{1}}\mathbf{B}_\mathbf{a}^\mathbf{T}\mathbf{P} \tag{24}$$

where $\mathbf{P}$ is the solution of the *generalized Riccati equation*, as follows:

$$\mathbf{A_a}^\mathrm{T}\mathbf{P} + \mathbf{P}\mathbf{A_a} - \mathbf{P}\mathbf{B_a}\mathbf{R}^{-1}\mathbf{B_a}^\mathrm{T}\mathbf{P} + \mathbf{Q} + \mathbf{L}^\mathrm{T}\mathbf{R}\mathbf{L} = \mathbf{0} \tag{25}$$

If the matrices ($\mathbf{R} > 0$ and $\mathbf{Q} > 0$) are chosen to satisfy the following conditions

$$\mathbf{R} = \frac{1}{1+\eta}\mathbf{I} \tag{26}$$

where $\eta > 0$ and

$$\mathbf{Q} \succ r\mathbf{S}^\mathrm{T}\mathbf{S} + \rho\mathbf{I} + \frac{1}{\eta}\mathbf{L}^\mathrm{T}\mathbf{L} \tag{27}$$

where $r > 0$ and $\rho > 0$, then the closed-loop system will be quadratically stable under the structural uncertainties described as $\Delta\mathbf{A_a} = \mathbf{B_a}\mathbf{S}$. Notice that conditions (26) and (27) are only valid when there are no uncertainties associated with the control input matrix ($\mathbf{B_a}$). Also, conditions $r > 0$ and $\rho > 0$ are imposed to guarantee that the matrix $\mathbf{Q}$ is positive definite and not positive semidefinite, as shown by Jabbari and Schmitendorf (1990). The solution of the *generalized Riccati equation* can be solved using the procedure proposed by Geromel and Peres (1985) if the state weighting matrix satisfies (26) and (27).

3.3 Proposed Procedure Based on the Riccati Equation

The application of the proposed design procedure can be summarized as follows:

Step 1: Define the order and the poles of the controller and build the matrices $\mathbf{A_c}$ and $\mathbf{C_c}$ in the canonical form;
Step 2: Define the matrices $\mathbf{A}$, $\mathbf{B}$ and $\mathbf{C}$ for all N operating points and define $\epsilon > 0$;
Step 3: Define the value of $\eta > 0$ and $\mathbf{R}$ as (26);
Step 4: Determine $\mathbf{\Delta A}$ from the set of N operating points;
Step 5: Calculate $\mathbf{S} = (\mathbf{B_a}^\mathrm{T}\mathbf{B_a})^{-1}\mathbf{B_a}^\mathrm{T}\Delta\mathbf{A_a}$;
Step 6: Define $r > 0$, $\rho > 0$ and calculate $\mathbf{Q_0} = r\mathbf{S}^\mathrm{T}\mathbf{S} + \rho\mathbf{I}$;
Step 7: Define $k = 0$ and $\mathbf{L_0} = 0$ and solve the Riccati equation $\mathbf{A_a}^\mathrm{T}\mathbf{P_0} + \mathbf{P_0}\mathbf{A_a} - \mathbf{P_0}\mathbf{B_a}\mathbf{R}^{-1}\mathbf{B_a}^\mathrm{T}\mathbf{P_0} + \mathbf{Q_0} = \mathbf{0}$ in $\mathbf{P_0}$;
Step 8: Set $k = k + 1$ and calculate

$$\mathbf{L}_k = \mathbf{R}^{-1}\mathbf{B_a}\mathbf{P}_{k-1}(\mathbf{I} - \mathbf{C_a}^\mathrm{T}(\mathbf{C_a}\mathbf{C_a}^\mathrm{T})^{-1}\mathbf{C_a}) \tag{28}$$

$$\mathbf{Q}_l = \frac{\mathbf{L}_k^\mathrm{T}\mathbf{L}_k}{\eta} \tag{29}$$

$$\mathbf{Q}_k = \mathbf{Q_0} + \mathbf{Q}_l \tag{30}$$

Step 9: Solve the Riccati equation in $\mathbf{P}_k$

$$\mathbf{A_a}^\mathrm{T}\mathbf{P}_k + \mathbf{P}_k\mathbf{A_a} - \mathbf{P}_k\mathbf{B_a}\mathbf{R}^{-1}\mathbf{B_a}^\mathrm{T}\mathbf{P}_k + \mathbf{Q}_k = \mathbf{0} \tag{31}$$

Step 10: If $||\mathbf{L}_k - \mathbf{L}_{k-1}|| < \epsilon$, go to Step 11. Otherwise go to Step 8;
Step 11: Calculate $\mathbf{K} = \mathbf{R}^{-1}\mathbf{B_a}^\mathrm{T}\mathbf{P}_{k-1} - \mathbf{L}_k$ and $\mathbf{G_a} = \mathbf{K}\mathbf{C_a}^\mathrm{T}(\mathbf{C_a}\mathbf{C_a}^\mathrm{T})^{-1}$;
Step 12: Determine $\mathbf{B_c}$ and $\mathbf{D_c}$ through

$$\mathbf{G_a} = \begin{bmatrix} -\mathbf{D_c} & -\mathbf{B_c} \end{bmatrix}^\mathrm{T} \tag{32}$$

4 Application of the Proposed Procedure to Design of Damping Controllers for Power Systems

In this section the selection of the poles of controllers, range of uncertainties and weighting matrices are discussed. First, the selection of the poles of the controller, performed in Step 1, affects the algorithm convergence for specific design requirements. There is no formal procedure for selecting the poles. Usually, the poles of damping controllers are located on the real axis of the left-hand side of the complex plane. In this paper, the poles were chosen to lie in the range of -1 to -100. If the algorithm fails to converge with the poles in this initial range, then the range may be extended to include a larger region of the complex plane, including complex poles with negative real parts. It is important to emphasize, however, that there is no particular constraint requiring that a controller pole has a multiplicity higher than one. Additionally, the methodology can be applied to re-tune the existing stabilizers in the system for the purpose of improving of the oscillation damping factor under several different operating conditions. In this case, the poles of the existing system stabilizers can be selected for use as controllers.

In Step 4, the system uncertainties must be defined. The strong requirement is that uncertainties must satisfy the following matching condition $\Delta\mathbf{A_a} = \mathbf{B_a S}$ (Trinh and Aldeen 1993). In this work, the main assumption is to cover the range of uncertainties at selected operating points. This procedure guarantees that the closed-loop system will be quadratically stable. On the other hand, this is clearly a conservative design assumption, because the entire range of uncertainties will not be reached during the regular power system operation. Since only load variation cases were considered, all the elements from the set of linear systems considered are between the extreme load variation cases (maximum–minimum load variation). In practice, we set $\mathbf{A}$ to be equal to the one extreme case (maximum load) and $\mathbf{\Delta A}$ to be the absolute difference between the elements of the other extreme case (minimum load).

Regarding the definition of the weighting matrices in Step 6, the method performance relied on weighting the matrices $\mathbf{Q}$ and $\mathbf{R}$; the performance considering uncertainties relies on setting the parameters η, r and ρ. This is unlike the method outlined in Costa et al. (1997), in which performance relied on weighting the matrices $\mathbf{Q}$ and $\mathbf{R}$. The parameter η must be a positive real number to guarantee that matrices $\mathbf{Q}$ and $\mathbf{R}$ are both positive definite. Its influence in the control weighting matrix $\mathbf{R}$ ensures the uniformity for all control devices. To avoid numerical problems, Trinh and Aldeen (1993) also recommend to increase the value of η in order to reduce the rate of change of $\mathbf{Q}_l$ during the convergence process. In the current work, the typical value of this parameter is greater than 100. Parameter r, meanwhile, is relative to the maximum bound for the uncertainties. Parameter ρ is used to weight $\mathbf{Q_0}$ so that it has more influence than $\mathbf{Q}_l$. When parameter ρ is larger than η, the influence of $\mathbf{Q_0}$ in $\mathbf{Q}$ increases. The typical parameters used for this control design are $\eta = 200$, $r = 7$ and $\rho = 0.01$.

5 Tests and Results

The applicability of the proposed design procedure is illustrated in two different test systems, with different size and control design challenges: the Brazilian equivalent system and the New England test system. Both systems are included in the set of IEEE benchmark test systems proposed in Canizares (2017). The design method chosen by Canizares (2017) is the gain and phase compensation approach which is widely used by utilities (Larsen and Swann 1981). Additionally, decentralized controllers were designed by the standard Riccati approach proposed by Costa et al. (1997) for a comparison analysis. In order to clarify the terminology that is adopted in this section, the standard Riccati method will be referred to as the LQR method, while the design procedure proposed in this paper will be referred to as the R-LQR method.

5.1 The Brazilian Equivalent System

The first test system is the Brazilian equivalent system, as shown in Fig. 1. It is a 7-bus, 5-machine equivalent model of the South/Southeastern Brazilian system configuration, in which the generator in Bus 7 is an equivalent of the Southeastern area (Canizares 2017). This system presents two inter-area modes: (a) the Southeastern equivalent system oscillating against the Itaipu power plant and (b) Southern system, which is composed by Salto Santiago, Salto Segredo and Foz do Areia power plants oscillating against the Southeastern equivalent system and the Itaipu power plant. This system requires damping controllers to operate in a stable way and with good performance.

Using the control schemes and settings described in Canizares (2017), the loads were varied by ± 5 and $\pm 10\%$, which created five operating conditions. (The base case and four additional cases with the loads increased and decreased by 5 and 10% from the base case.) Additionally, using the same control scheme and controller poles described in Canizares (2017), a decentralized controller was designed following the LQR method, which is the design procedure proposed by Costa et al. (1997).

The modal analysis of these five operating conditions was performed with PacDyn (CEPEL 2015) for the controllers tuned as presented in Canizares (2017) and for those designed according to the LQR method. The results for the most poorly damped oscillation mode are presented in Table 1. For the

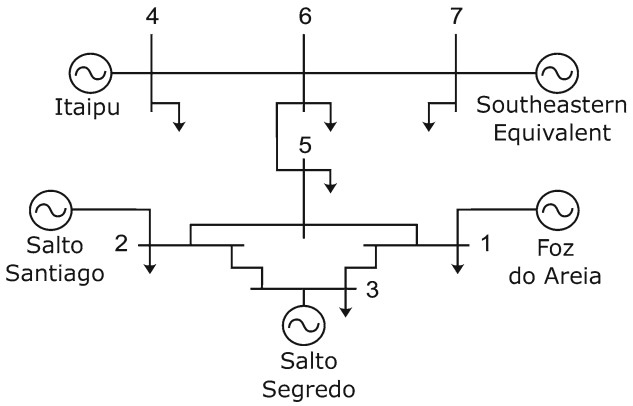

Fig. 1 IEEE Brazilian equivalent system

Table 1 Poorly damped oscillatory modes

Case	Benchmark		LQR	
	$\zeta(\%)$	f (Hz)	$\zeta(\%)$	f (Hz)
Base	6.39	0.83	7.09	1.66
Load + 5%	8.25	0.83	2.23	1.18
Load − 5%	4.39	0.82	2.49	0.99
Load + 10%	9.99	0.84	0.35	1.20
Load − 10%	2.25	0.81	− 1.8	0.97

controller proposed by Canizares (2017), the poorly damped mode is the inter-area mode (a), as defined previously, and the power system is stable for all five operating conditions. The modal performance is degraded when the load is reduced (− 5 and − 10%) because this increases the power transfer to the Southeastern system. In these cases, the oscillation mode crosses the minimum damping ratio of 5%. For the controller designed by the LQR method, the poorly damped mode is a local or an inter-area mode, depending on the operating condition. However, the power system is not stable for all five operating conditions. The modal performance became unstable when the load is decreased by − 10%.

5.1.1 Robust Design Via the Proposed R-LQR Method and Small-Signal Analysis

The same load conditions were considered for the control design proposed in this paper. The modal analysis of these five power system operating conditions was performed with PacDyn (CEPEL 2015). The results are presented in Table 2 for the most poorly damped oscillation mode. The analysis revealed that all oscillation modes present a damping ratio higher than 8% for the five selected operating conditions. Additionally, the eigenvalue locus for the modes corresponding to a set of 1900 operating conditions obtained from the convex combination of three closed-loop operating conditions (base case and the cases with the loads increased and decreased by 10%) is shown in Fig. 2. The main result of this exhaustive search is the finding that the oscillatory modes are not impaired under any operating condition presenting a damping ratio far higher than 5%. Table 3 presents the parameters of the decentralized controller designed according to the R-LQR method described in the previous sections.

Table 2 Poorly damped oscillation mode—damping controllers designed via the proposed R-LQR method

Case	$\zeta(\%)$	f (Hz)
Base	9.37	1.67
Load + 5%	9.25	1.67
Load − 5%	9.37	1.76
Load + 10%	9.15	1.68
Load − 10%	8.02	0.91

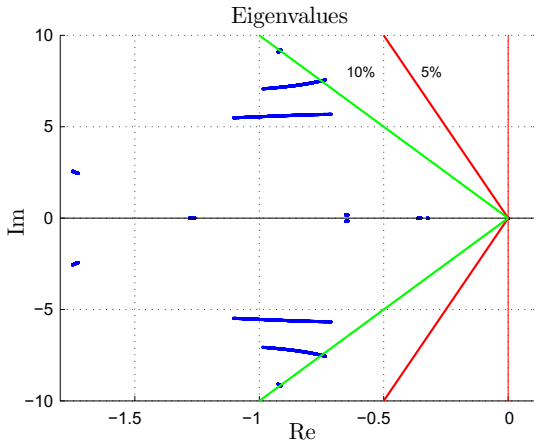

Fig. 2 Eigenvalue locus for the modes corresponding to a set of 1900 operating conditions obtained from the convex combination of three closed-loop operating conditions

Table 3 Parameters of the proposed decentralized controllers for the IEEE 7 bus system

	n_2	n_1	n_0	a_1	a_0
dc_1	− 14.16	170.7	1296	26.67	177.78
dc_2	46.38	752.4	1775	26.67	177.78
dc_3	32.73	1232	1519	26.67	177.78
dc_4	353.9	4477	− 2201	30.77	236.68

5.2 The New England Test System

The New England test system (NETS), shown in Fig. 3, has been extensively employed in the oscillation damping control literature (Canizares 2017; de Menezes et al. 2016). It comprises 39 buses and 10 generators. Generator 1 is an area-equivalent that represents the New York system to which the New England system is interconnected. Almost all electromechanical modes in this system are of a local or regional

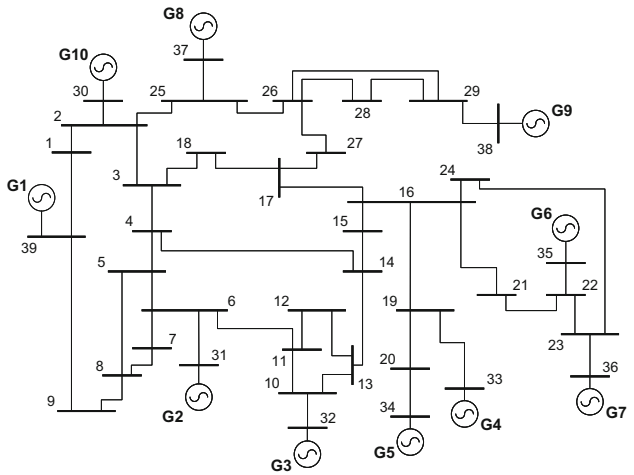

Fig. 3 New England test system (NETS)

Table 4 Relevant oscillatory modes—damping controllers tuned as presented in Canizares (2017)

Case	Mode 1		Mode 2		Mode 3	
	$\zeta(\%)$	f (Hz)	$\zeta(\%)$	f (Hz)	$\zeta(\%)$	f (Hz)
Base	13.4	0.58	18.14	1.59	18.15	1.13
+10	11.18	0.58	18.13	1.59	20.21	0.96
−10	12.70	0.58	18.12	1.59	0.05	0.94
Case	Mode 4		Mode 5		Mode 6	
	$\zeta(\%)$	f (Hz)	$\zeta(\%)$	f (Hz)	$\zeta(\%)$	f (Hz)
Base	18.19	1.36	23.42	1.0	23.47	1.68
+10	17.42	1.35	20.24	1.05	23.54	1.68
−10	20.37	1.32	23.8	1.0	23.44	1.68

nature, except for one, which is observed as the oscillation of generators 2 to 10 against generator 1.

Considering the control schemes (PSSs placed at every power plant) and settings described in Canizares (2017) to form the base case, the other two operating points were obtained by increasing and decreasing the loads by 10% from the base case. The modal analysis of these three operating conditions was performed with PacDyn (CEPEL 2015). The results are presented in Table 4, which shows six relevant oscillatory modes. All the other modes present damping ratio higher than ± 15% for all the considered designed methods. Mode 1 is the inter-area mode, which involves all generators against the area-equivalent given by the New York system. The other ones are multiple local modes that may be critical under certain operating conditions. Mode 3 is very well damped for the base case and for the operating condition given by an increase of 10% in the loads. However, this same mode became critical when the loads were reduced by 10%.

Table 5 Relevant oscillatory modes—damping controllers designed by the LQR methods

Case	Mode 1		Mode 2		Mode 3	
	$\zeta(\%)$	f (Hz)	$\zeta(\%)$	f (Hz)	$\zeta(\%)$	f (Hz)
Base	31.90	0.59	11.59	1.58	6.25	0.86
+10	31.09	0.59	11.59	1.58	6.25	0.86
−10	34.83	0.58	11.52	1.58	−1.91	0.88
Case	Mode 4		Mode 5		Mode 6	
	$\zeta(\%)$	f (Hz)	$\zeta(\%)$	f (Hz)	$\zeta(\%)$	f (Hz)
Base	8.21	1.42	12.35	1.38	12.34	1.36
+10	11.42	1.42	12.35	1.38	7.78	1.36
−10	9.74	1.42	14.10	1.34	5.09	1.37

Using the same poles and structure of controllers described in Canizares (2017), a decentralized controller for each generator was designed via the LQR method, which was the design procedure proposed in Costa et al. (1997). The results are presented in Table 5 for the same oscillatory modes shown in Table 4. Mode 3 is poorly damped for all cases and unstable when the loads are reduced by 10% from the base case.

5.2.1 Robust Design Via the Proposed R-LQR Method and Small-Signal Analysis

This subsection presents the results obtained from the application of the proposed design procedure. The modal analysis of the same three operating conditions considered in the last subsection was performed with PacDyn (CEPEL 2015). The results are presented in Table 6, which shows that the power system is stable for all three operating points. The modal performance is not impaired under any operating conditions, and all the modes present a damping ratio superior to 5%. The frequency of the inter-area mode varied from 0.58 to 0.40 Hz, and its damping is higher than 20% for all operating points. The critical oscillatory mode, Mode 3, presents damping ratio superior to 7% for all the cases. The transfer function parameters of the designed controllers are presented in Table 7.

5.2.2 Nonlinear Simulation

Nonlinear, time-domain simulations were carried out using ANATEM software (CEPEL 2014) in the New England test system in order to validate the results of the linear analysis and to ensure performance robustness for the designed damping controllers. The proposed damping controllers were compared to the available controllers in Canizares (2017) and the controllers designed by the traditional LQR method presented in Costa et al. (1997). A temporary, three-phase short

Table 6 Relevant oscillatory modes—damping controllers designed via the proposed R-LQR method

Case	Mode 1		Mode 2		Mode 3	
	$\zeta(\%)$	f (Hz)	$\zeta(\%)$	f (Hz)	$\zeta(\%)$	f (Hz)
Base	26.46	0.40	8.53	1.97	9.66	1.09
+10	31.14	0.40	8.60	1.96	7.88	0.80
−10	26.12	0.40	8.51	1.96	7.66	0.96
Case	Mode 4		Mode 5		Mode 6	
	$\zeta(\%)$	f (Hz)	$\zeta(\%)$	f (Hz)	$\zeta(\%)$	f (Hz)
Base	11.45	1.84	8.53	1.56	14.03	1.63
+10	11.54	1.82	8.47	1.57	14.11	1.64
−10	11.55	1.82	8.72	1.55	8.74	1.73

Table 7 Parameters of the proposed decentralized controllers for the IEEE 39 bus system

	n_2	n_1	n_0	a_1	a_0
dc_1	0.3612	4.196	3.399	3.67	3.33
dc_2	21.39	−194.3	−31.64	12.5	25.0
dc_3	194.2	873.2	48.34	10.0	25.0
dc_4	123.7	917.3	39.56	13.33	33.33
dc_5	135.8	2023	−56.64	15.0	50.0
dc_6	1.358	334.2	400	30.0	200.0
dc_7	35.35	11930	846.3	60.0	500.0
dc_8	72.77	626.5	26.91	15.0	50.0
dc_9	134.2	1001	35.72	12.0	20.0
dc_{10}	−74.97	−33	24.88	22.0	40.0

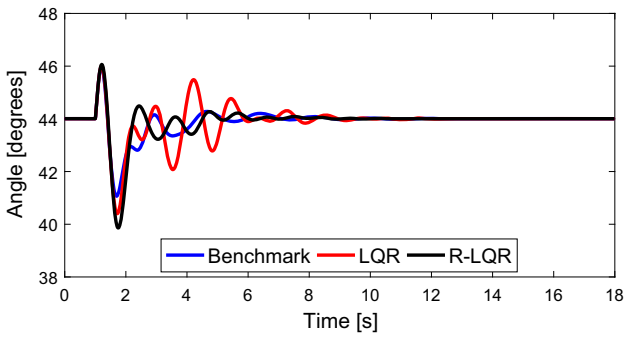

Fig. 4 Angle of generator 2, Bus 31

circuit of 10 ms was applied at Bus 31 and cleared without any switching. The angle and field voltage of generator 2 at Bus 31, for the base case, are presented in Figs. 4 and 5, respectively. Additionally, the angle and field voltage of generator 2 at Bus 31, for the load − 10% case, are presented in Figs. 6 and 7, respectively.

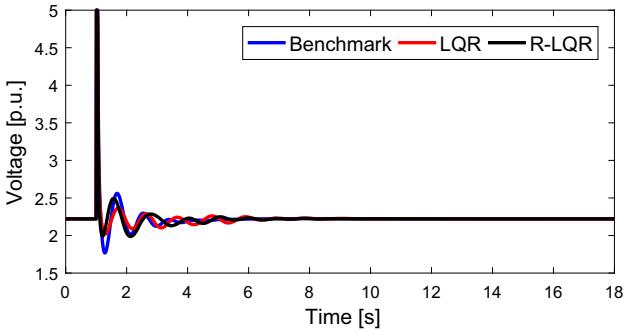

Fig. 5 Field voltage of generator 2, Bus 31

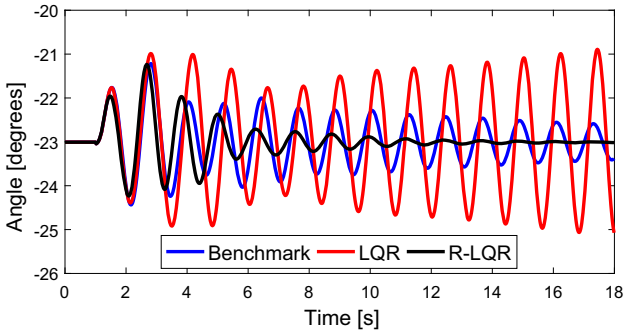

Fig. 6 Angle of generator 2, Bus 31

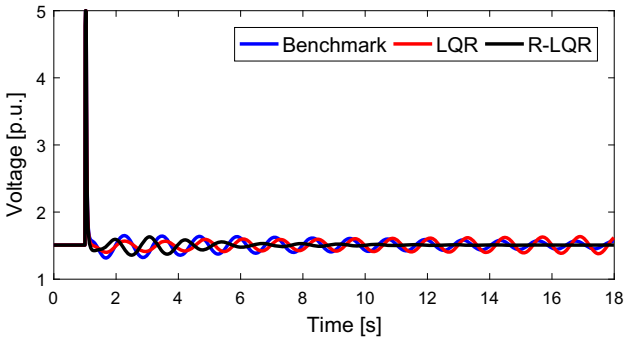

Fig. 7 Field voltage of generator 2, Bus 31

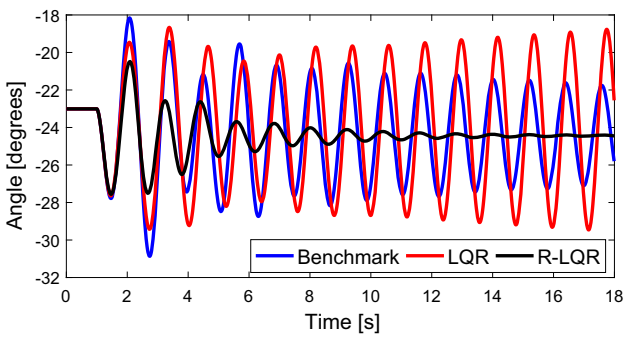

Fig. 8 Angle of generator 2, Bus 31

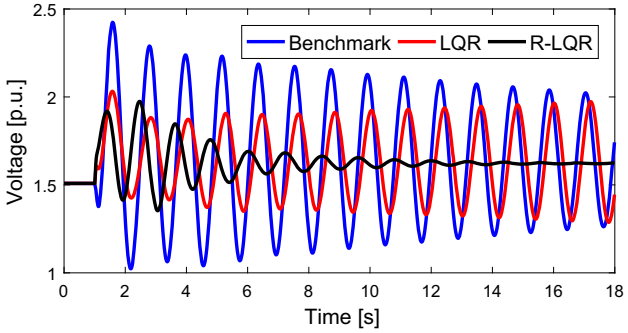

Fig. 9 Field voltage of generator 2, Bus 31

Another nonlinear simulation included the contingency given by a permanent disconnection of the transmission line 6–11 in $t = 1$ s. The rotor angle and field voltage of generator 2 at Bus 31 for the worst case are presented in Figs. 8 and 9, respectively. The angular and field voltage responses for the power system equipped with the proposed decentralized controllers were better damped than the responses for the system with the controllers tuned as presented in Canizares (2017) and Costa et al. (1997). Hence, the robust controllers presented a coordinated control action and a satisfactory performance.

6 Conclusions

This paper presents a robust coordination approach for designing decentralized controllers to stabilize multiple low damping oscillation modes. The resulting controller guarantees quadratic stability for the specified range of uncertainties. The conventional decentralized control scheme was chosen because it is a challenging problem, making it a good choice for method evaluation. However, the design procedure could be regarded as the guideline for other power system control design problems (Dotta et al. 2009). Test results in the two IEEE benchmarks show that the method is effective. The modal analysis indicates the control robustness for different operating points at a range of uncertainties. Furthermore, a nonlinear simulation is performed verifying the presented method concept and the designed decentralized controller under various operating conditions. All of the research results indicate that the proposed robust coordination approach may contribute to effective damping in low damping oscillations and present robustness under various operating conditions. No model reduction methods were applied in the system and resulting controller. Future work will include methods to relax the matching condition specified in the original algorithm.

Acknowledgements The authors gratefully acknowledge the permission of CEPEL for the use of ANATEM and PacDyn and wish to acknowledge with thanks Prof. Aguinaldo S. Silva for carefully reading this paper.

References

Annaswamy, A. M., & Amin, M. (2013). *IEEE vision for smart grid controls: 2030 and beyond. IEEE vision for smart grid controls: 2030 and beyond* (pp. 1–168).

Apkarian, P., Noll, D., & Rondepierre, A. (2007). Nonsmooth optimization algorithm for mixed H_2/H_{inf} synthesis. In: *2007 46th IEEE conference on decision and control* (pp. 4110–4115). IEEE. https://doi.org/10.1109/CDC.2007.4434088.

Bian, X. Y., Geng, Y., Lo, K. L., Fu, Y., & Zhou, Q. B. (2016). Coordination of PSSs and SVC damping controller to improve probabilistic small-signal stability of power system with wind farm integration. *IEEE Transactions on Power Systems*, *31*(3), 2371–2382. https://doi.org/10.1109/TPWRS.2015.2458980.

Canizares, C., et al. (2017). Benchmark models for the analysis and control of small-signal oscillatory dynamics in power systems. *IEEE Transactions on Power Systems*, *32*(1), 715–722. https://doi.org/10.1109/TPWRS.2016.2561263.

Castoldi, M. F., Sanches, D. S., Mansour, M. R., Bretas, N. G., & Ramos, R. A. (2014). A hybrid algorithm to tune power oscillation dampers for FACTS devices in power systems. *Control Engineering Practice*, *24*, 25–32. https://doi.org/10.1016/j.conengprac.2013.11.001.

CEPEL. (2014). Anatem user's manual version 10.5.2 Available: http://www.dre.cepel.br/.

CEPEL. (2015). PacDyn documentation. Available: http://www.pacdyn.cepel.br.

Costa, A. J. A. S., Freitas, F. D., & e Silva, A. S. (1997). Design of decentralized controllers for large power systems considering sparsity. *IEEE Transactions on Power Systems*, *12*(1), 144–152. https://doi.org/10.1109/59.574934.

de Menezes, M. M., de Araujo, P. B., & do Valle, D. B. (2016). Design of PSS and TCSC damping controller using particle swarm optimization. *Journal of Control, Automation and Electrical Systems*, *27*(5), 554–561. https://doi.org/10.1007/s40313-016-0257-z.

Deng, J., & Zhang, X. P. (2014). Robust damping control of power systems with TCSC: A multi-model bmi approach with H_{inf} performance. *IEEE Transactions on Power Systems*, *29*(4), 1512–1521. https://doi.org/10.1109/TPWRS.2013.2292067.

Do Bomfim, A. L. B., Taranto, G. N., & Falcao, D. M. (2000). Simultaneous tuning of power system damping controllers using genetic algorithms. *IEEE Transactions on Power Systems*, *15*(1), 163–169. https://doi.org/10.1109/59.852116.

Dotta, D., e Silva, A. S., & Decker, I. C. (2009). Wide-area measurements-based two-level control design considering signal transmission delay. *IEEE Transactions on Power Systems*, *24*(1), 208–216. https://doi.org/10.1109/TPWRS.2008.2004733.

Elkington, K., & Ghandhari, M. (2013). Non-linear power oscillation damping controllers for doubly fed induction generators in wind farms. *IET Renewable Power Generation*, *7*(2), 172–179. https://doi.org/10.1049/iet-rpg.2011.0145.

Galvan, F., & Overholt, P. (2014). The intelligent grid enters a new dimension. *Transmission and Distribution World*, *66*(8), 22–29.

Geromel, J. C., & Peres, P. L. D. (1985). Decentralised load-frequency control. *IEE Proceedings D Control Theory and Applications*, *132*(5), 225. https://doi.org/10.1049/ip-d.1985.0039.

Jabbari, F., & Schmitendorf, W. E. (1990). A noniterative method for the design of linear robust controllers. *IEEE Transactions on Automatic Control*, *35*(8), 954–957. https://doi.org/10.1109/9.58512.

Kundur, P. (1994). *Power System Stability and Control* (Vol. 7). New York: McGraw-hill.

Larsen, E. V., & Swann, D. A. (1981). Applying power system stabilizers part ii: Performance objectives and tuning concepts. *IEEE Transactions on Power Apparatus and Systems PAS*, *100*(6), 3025–3033. https://doi.org/10.1109/TPAS.1981.316410.

Lu, C. F., Hsu, C. H., & Juang, C. F. (2013). Coordinated control of flexible AC transmission system devices using an evolutionary fuzzy lead-lag controller with advanced continuous ant colony optimization. *IEEE Transactions on Power Systems*, *28*(1), 385–392. https://doi.org/10.1109/TPWRS.2012.2206410.

Ortega, A., & Milano, F. (2016). Generalized model of VSC-based energy storage systems for transient stability analysis. *IEEE Transactions on Power Systems*, *31*(5), 3369–3380. https://doi.org/10.1109/TPWRS.2015.2496217.

Ramos, R. A., Alberto, L. F. C., & Bretas, N. G. (2004). A new methodology for the coordinated design of robust decentralized power system damping controllers. *IEEE Transactions on Power Systems*, *19*(1), 444–454. https://doi.org/10.1109/TPWRS.2003.820690.

Shahgholian, G., & Movahedi, A. (2016). Power system stabiliser and flexible alternating current transmission systems controller coordinated design using adaptive velocity update relaxation particle swarm optimisation algorithm in multi-machine power system. *IET Generation, Transmission & Distribution*, *10*(8), 1860–1868. https://doi.org/10.1049/iet-gtd.2015.1002.

Trinh, H., & Aldeen, M. (1993). Decentralised feedback controllers for uncertain interconnected dynamic systems. *IEE Proceedings D Control Theory and Applications*, *140*(6), 429. https://doi.org/10.1049/ip-d.1993.0056.

Wilches-Bernal, F., Lackner, C., & Chow, JH. (2016). Power system controllability through nontraditional generation. In: *2016 IEEE 55th conference on decision and control (CDC)* (pp 702–708)